Asian Journal of Chemistry; Vol. 29, No. 12 (2017), 2776-2780

ASIAN JOURNAL OF CHEMISTRY

https://doi.org/10.14233/ajchem.2017.20896

Characterization and Magnetic Behaviour of Nanosized Binary Spinel Ferrites Synthesized by Low Temperature Hydrothermal Method and their Stability in Aqueous Suspensions

V. BEULA SHANTHI AMMANI AMMAL[1,*], N. JOHN JEBARATHINAM[2] and D. JAYALAKSHMI[3]

[1]Department of Physics, Jerusalem College of Engineering, Narayanapuram, Chennai-600 100, India
[2]Department of Chemistry, Jerusalem College of Engineering, Narayanapuram, Chennai-600 100, India
[3]Department of Physics, Queen Mary's College, Chennai-600 004, India

*Corresponding author: E-mail: beulashanthijohn@rediffmail.com

Received: 30 June 2017; *Accepted*: 28 July 2017; *Published online*: 30 October 2017; AJC-18632

Cobalt ferrite, nickel ferrite and zinc ferrite spinel oxides are synthesized by low temperature hydrothermal method using ethylenediamine tetracetic acid (EDTA) as complexing agent. FTIR and XRD studies show the formation of pure and single spinel phase. The average crystalline size was determined from X-ray diffraction line broadening using Scherrer equation. FE-SEM studies revealed that all the synthesized ferrites are having nearly octahedron crystals with an average particle size of 20 to 40 nm. Magnetic behavior of cobalt ferrite, nickel ferrite and zinc ferrite spinels studied by vibrating sample magnetometer at room temperature shows ferromagnetic behaviour of cobalt ferrite, super paramagnetic nature of nickel ferrite and non-magnetic behaviour of zinc ferrite. Zeta potential measured at various pH conditions shows that cobalt ferrite and nickel ferrite can be used for the preparation of magnetic nanofluids with stable colloidal dispersion at 4.5 > pH < 7.5 and 3.5 > pH < 9.5, respectively.

Keywords: Hydrothermal, Spinel ferrites, Nanoparticles, Zeta potential, Nanofluids, Super-paramaganetism.

INTRODUCTION

Ferro spinel compounds possess high permeability so that they can be used in electronics [1-3], in microwave and high density information storage devices [4], as ferrofluids [5] and magnetic drug delivery materials [6], *etc*. Spinel ferrites, possessing cubically close packed array of oxygen anions with the metallic ions occupy two crystallographically different sites, *i.e*. octahedral [B] and tetrahedral (A) site. Three kind of magnetic interactions are possible, between metallic ions, through the intermediate O^{2-} ions, by super-exchange mechanism, namely, A-A interaction, B-B interaction and A-B interaction. It has been established experimentally that these interaction energies are negative and hence induce an anti-parallel orientation.

Due to the specific electronic configurations of cations and the types of super-exchange interactions among them, the magnetic properties of ferrites are strongly dependent on the occupancy and exchange of cations in the two sites. In spinel ferrites, direct interactions are negligible, due to the large distance between cations. Super-exchange interaction occurs between two metal cations through the existence of a bridging oxygen ion. It involves the temporary transfer of one oxygen 2*p* electron to a neighboring metal ion. The A-B interaction is the strongest super-exchange interaction in the spinel structure, followed by B-B interaction, and then A-A interaction. The magnetic properties of spinel ferrites are also influenced by the particle size and their distribution [7,8]. Hence synthesis of spinel ferrites under suitable conditions to attain uniform octahedron structure with nanosize particle size will help to study the influence of magnetic properties with respect to exchange interactions between A and B cations and also the particle size and their distribution. Rajput *et al*. [9] used ethylene diammine tetraacetic acid (EDTA) as complexing agent for the synthesis of nanosized simple binary spinel ferrites with uniform octahedron structure. Rahal *et al*. [10] studied the role of EDTA as capping agent on structure and established that EDTA assist the formation of uniform and significant size reduction of nanoparticles. In the present investigation three binary spinel ferrites having inversed (nickel ferrite), partially inversed (cobalt ferrite) and normal (zinc ferrite) spinel structure are synthsized by low temperature, hydrothermal method assisted by ethylene diammine tetraacetic acid (EDTA) as complexing agent. Spinel phase formation, particle size and their distributions are determined by XRD and FESEM analysis. Vibrating sample magnetometer (VSM) studies on all these materials are carried out at room temperature to understand the magnetic behaviour and their relation to cation distribution in A and B sites, particle size and their distribution.

In recent years, nanofluids prepared using nanoferrite materials find wide applications in heat transfer, microelectronics, biomedical processes, *etc*. [11-13]. When nanoparticles are in a liquid carrier the first problem that needs to be solved is their clustering and precipitation, especially in a magnetic fluid. Zeta potential is an important parameter reflecting the colloid behaviour of the particles [14]. In the present study, nanofluid of as-synthesized spinel ferrites using water as base fluid are prepared and their stability are investigated by measuring Zeta potential at various pH conditions.

EXPERIMENTAL

For the synthesis of cobalt ferrite, nickel ferrite and zinc ferrite stoichiometric amounts of Analar grade cobalt chloride, nickel chloride, zinc chloride and ferric chloride in M:Fe molar ratio of 1:2 (where M = Co, Ni or Zn) were weighed and each of which was dissolved in 50 mL of a solution containing 0.5 g of disodium salt of ethylene diammine tetraacetic acid (EDTA) with constant stirring by magnetic stirrer. Sodium hydroxide solution (4.4 mol) was added dropwise into each mixture till the pH is increased to 12. The precipitate produced was stirred for another 3 h at room temperature. Then the precipitate was transferred into an autoclave (23 mL capacity) and kept at 120 ºC for 12 h in an air oven. The precipitate obtained was centrifuged and washed with distilled water and ethanol.

It was then dried at 100 ºC for 6 h. Aqueous solutions of 0.01 % of as-synthesized spinel ferrites are prepared to obtain nanofluids. pH of the nanofluids ranging from 3 to 10 are maintained by the addition of suitable buffer solutions. The solution was sonicated for 30 min in order to prevent particle agglomeration before measuring Zeta potential. Zeta potential of the prepared nanofluids are measured using NanoZS (Malvern UK) employing a 532 nm laser at a back scattering angle of 173º.

Characterization: Powder X-ray diffraction (XRD) patterns were measured by using RICH-SIEFERT 3000-TT diffractometer employing Cu Kα radiation. The Fourier transform infrared (FTIR) was performed by KBr tablet method in the range 4000-250 cm^{-1} in a BRUKER model IFS 66 V FTIR spectrometer. The morphologies of the samples were examined with field emission scanning electron microscope (FESEM, FEI Nova-Nano SEM-600, The Netherlands). Magnetic measurements were performed by Quantum design SQUID vibrating sample magnetometer (VSM) at room temperature.

RESULTS AND DISCUSSION

The FTIR spectra of synthesized spinel ferrites are given in Fig.1. The vibrational spectra of absorption bands were observed only in the range between 330 to 610 cm^{-1} which are characteristic to spinel structure of the synthesized ferrites [15]. The absorption bands observed at 330 and 531 cm^{-1} for cobalt ferrite, 480 and 602 cm^{-1} for nickel ferrite and 412 and 571 cm^{-1} for zinc ferrite are due to the vibrations of octahedral metal-oxygen bond and tetrahedral metal-oxygen bond, respectively. The absence of peaks at 1300-1000 and 3000-2000 cm^{-1} shows non-existence of O-H mode, C-O mode and C=H stretching-mode of vibrations, respectively. This FTIR analysis confirms the method of low temperature hydrothermal synthesis using EDTA as complexing agent results in the formation of pure spinel ferrites.

The XRD pattern of the synthesized ferrites are shown in Fig. 2, which exhibit typical reflections of (220), (311), (222),

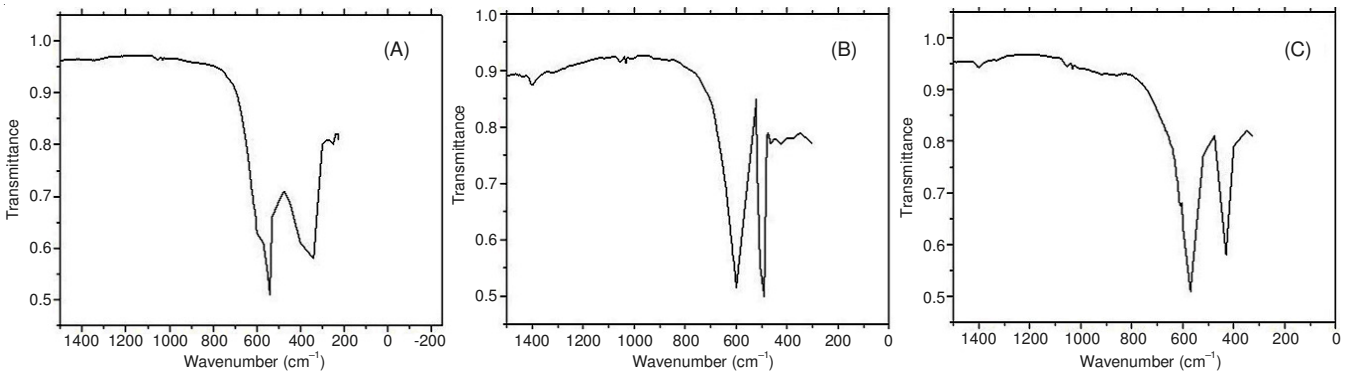

Fig. 1. FTIR spectra of cobalt ferrite (A), nickel ferrite (B), zinc ferrite (C)

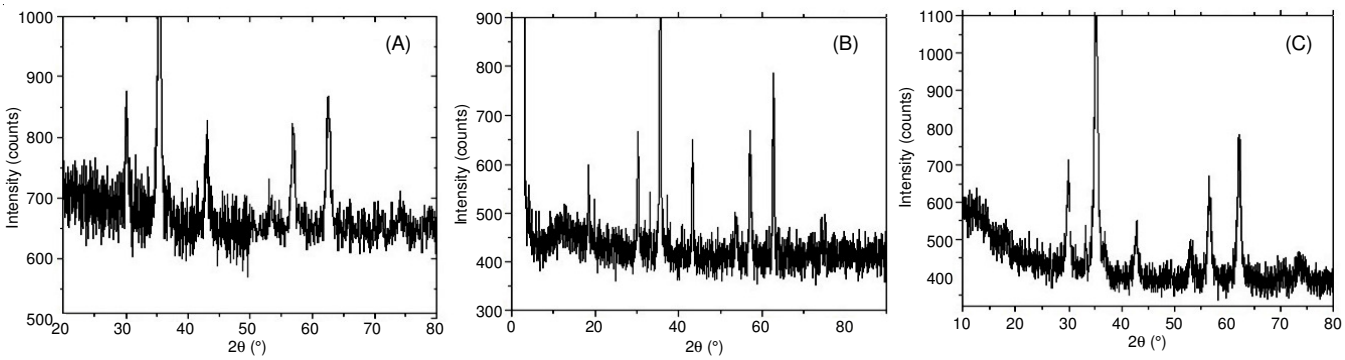

Fig. 2. XRD spectra of cobalt ferrite (A), nickel ferrite (B), zinc ferrite (C)

(400), (422), (511) and (440) planes that are indications of the presence of the cubic spinel structure. All of the diffraction peaks match well with the reported values (JCPDS File No. 22-1086 for cobalt ferrite, File No:10-0325 for nickel ferrite, and File No.22-1012 for zinc ferrite).

The average crystal size is determined by Scherrer equation using the peak broadening (FWHM) of the most intense peak (311): $t = 0.9\lambda/\beta\cos\theta$; where λ is the wavelength of CuKα (1.54059 Å), θ is the angle of Bragg diffraction at full width half maximum (FWHM). The average crystallite size obtained for all the spinel ferrites are given in Table-1.The cation distribution at A and B sites are determined by X-ray intensity calculations following the method reported by Jebarathinam *et al*. [16].

The morphology obtained by FESEM analysis (Fig. 3) shows incomplete octahedron structures for all the synthesized ferrites. The addition of EDTA controls the size as well as the shape of nanoparticles and prevents their agglomeration. The average crystal size observed from FESEM images are in good agreement with the calculated values by XRD. Lattice constant (a) and volume of unit cell (a^3) are also calculated for cobalt, nickel and zinc ferrite (Table-1).

The hysteresis curve for cobalt ferrite, nickel ferrite and zinc ferrite at room temperature are given in Fig. 4. The magnetic parameters values are given in Table-2. Hysteresis loop for $NiFe_2O_4$ (Fig. 4b) is typical for soft magnetic materials and the "S" shape of the curve with the zero coercivity and saturation magnetization Ms = 30 emu/g indicate the presence of small magnetic particles exhibiting super-paramagnetic behaviour.

TABLE 2
MAGNETIC PARAMETERS AND ISOELECTRIC POINT OF SPINEL FERRITES

Sample	Coercivity (Oe)	Retentivity (emu/g)	Saturation magneti-zation (emu/g)	Isoelectric point (pH)
Cobalt ferrite	580	25	60	6.3
Nickel ferrite	0	18	38	7.4
Zinc ferrite		Non-magnetic		4.5

The magnetic properties of $NiFe_2O_4$ with an inverse spinel structure can be explained in terms of the cations distribution at tetrahedral [A] and octahedral [B] sites. Cation distribution (Table-1) shows that $NiFe_2O_4$ exhibits inverse spinel structure with all bivalent Ni^{2+} present at tetrahedral sites [A] along with half of the trivalent Fe^{3+} ions and the remaining half of the trivalent Fe^{3+} present at the octahedral sites [B]. Fe^{3+} has a magnetic moment of 5.9 μ_B and Ni^{2+} has a magnetic moment of 3.2 μ_B. The antiparallel arrangement cancels the moments of Fe^{3+} in octahedral and tetrahedral sites. The net moment therefore only comes from the magnetic moment of Ni^{2+}, which is parallel to Fe^{3+} in octahedral sites. Nejati and Zabihi [17] reported that change from ferromagnetism to super paramag-

TABLE 1
CRYSTAL PARAMETER AND CATION DISTRIBUTION IN SPINEL FERRITES

Sample	Lattice constant (a) Å	Volume of unit cell (a^3) Å^3	Average size from XRD (nm)	Average size from FESEM (nm)	Cation distribution	
					A site	B site
Cobalt ferrite	8.44	601.21	33.28	26.38	0.25 Co^{2+}, 0.75 Fe^{3+}	0.75 Co^{2+}, 1.25 Fe^{3+}
Nickel ferrite	8.36	584.27	33.42	28.44	Fe^{3+}	Ni^{2+}, Fe^{3+}
Zinc ferrite	8.44	601.24	16.69	22.78	Zn^{2+}	2Fe^{3+}

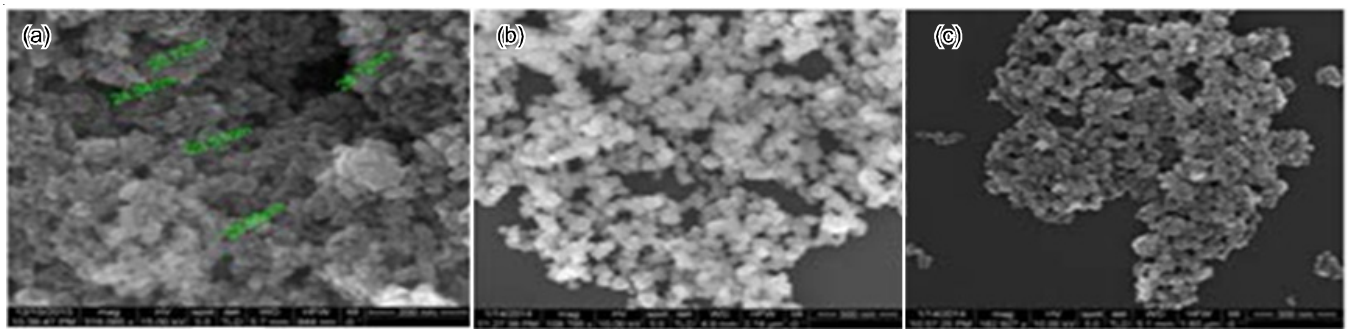

Fig. 3. Field emission scanning microscopy images of (a) cobalt ferrite (b) nickel ferrite (c) zinc ferrite

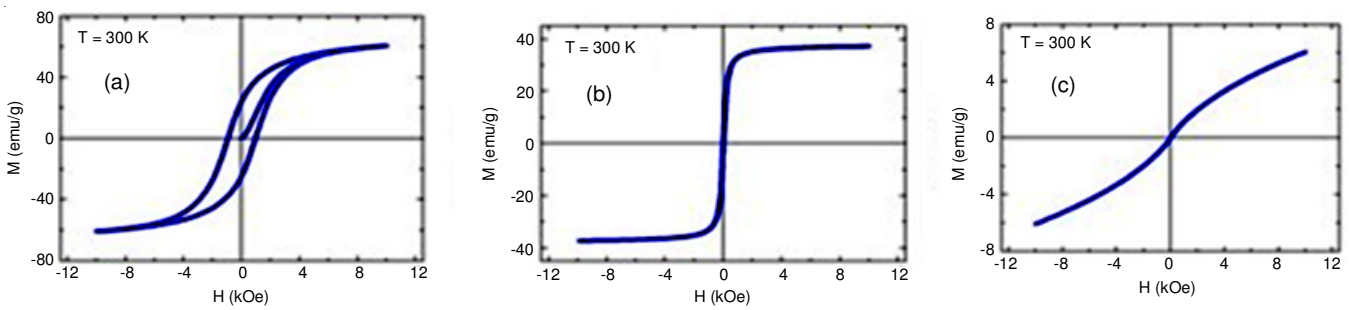

Fig. 4. Hysteresis curve of (a) cobalt ferrite (b) nickel ferrite (c) zinc ferrite

netism of nickel ferrite is attributed to its particle size. As the diameter of the synthesized nickel ferrite nonparticles is less than 30 nm, nickel ferrite show the character of super-paramagnetism. In super-paramagnetic $NiFe_2O_4$, responsiveness to an applied magnetic field without retaining any magnetism after removal of the magnetic field is observed. This behaviour is an important property for using $NiFe_2O_4$ as magnetic targeting carriers.

The magnetic studies of cobalt ferrite show a ferromagnetic behaviour with coercivity 580 Oe and saturation magnetization 60 emu/g (Fig. 4a). As the cobalt ferrite is partially inverse only 0.75 Co^{2+} are present along with 1.25 Fe^{3+} in octahedral sites (Table-1). However, the higher magnetic moment of Co^{2+} (4.7 μ_B) compare to Ni^{2+} (3.2 μ_B) is attributed to the observed higher saturation magnetization (60 emu/g) for cobalt ferrite. The moderate saturation magnetization and low coercivity of cobalt ferrite is important for hyperthermia method of cancer treatment and also other biomedical applications [18]. Magnetic studies of zinc ferrite show non-magnetic behaviour at room temperature (Fig. 4c). As given in Table-1, zinc ferrite has normal spinel structure with all divalent Zn^{2+} ions present at tetrahedral sites (A) and all Fe^{3+} ions present at octahedral sites (B). As Fe^{3+} on octahedral sites are in anti-parallel order through B-B interaction and Zn^{2+} has zero magnetic moment, zinc ferrite has zero net magnetic moment.

Variation of zeta potential measured at various pH conditions for as-synthesized cobalt ferrite, nickel ferrite and zinc ferrite nanofluides are shown in Fig. 5. The isoelectric points at which the surfaces of nanoparticles do not carry any charge are given in Table-2. At the pH corresponding to isoelectric point, particles inside the fluid would be tend to agglomerate. However, when zeta potential of the particle is farther away from the isoelectric point, better the dispersion ability. It is observed from Fig. 5 that the maximum positive zeta potential of +60 mV and maximum negative zeta potential of -72 mV was obtained at pH 3 and 10, respectively for cobalt ferrite. The corresponding values for nickel ferrite is found to be +43 mV and -41 mV and for zinc ferrite the values are +20 mV and -27 mV, respectively.

As cobalt ferrite and nickel ferrite nanofluids have zeta potential more than 30 mV (+ or -) at pH range 4.5 > pH < 7.5 and 3.5 > pH < 9.5, respectively prevent aggregation of nanoparticles and provide excellent stability. The magnitude and sign of zeta potential on nanoparticle surface is a very important consideration in targeted drug delivery processes [19,20]. Knowledge on zeta potential of uncoated nanoparticles in aqueous medium helps to optimize conditions for surface modification with biodegradable polymers to synthesis biocompatible nanoparticles.

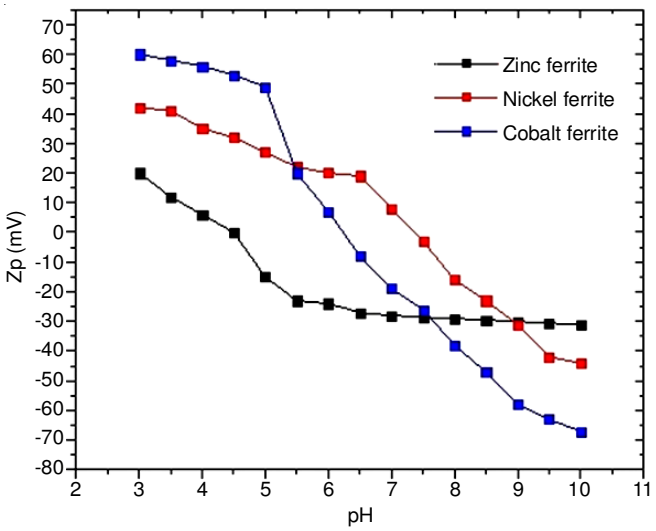

Fig. 5. Variation of zeta potential with pH of as-synthesized ferrite nano fluids

Conclusion

FTIR study shows EDTA assisted low temperature hydrothermal synthesis of cobalt ferrite, nickel ferrite and zinc ferrite is a suitable method for obtaining nano size spinel ferrites with pure and singles spinel phase . The average crystallite size obtained by XRD and FESEM analysis indicate significant size reduction in ferrite particles. The magnetic studies demonstrate the ferromagnetic behaviour of cobalt ferrite, super-paramantic nature of nickel ferrite and nonmagnetic behaviour of zinc ferrite. The magnetic moments of cations distributed between octahedral and tetrahedral sites in the spinel structure are correlated to the magnetic characteristics of the synthesized ferrites. Nanofluids prepared using as-synthesised spinel ferrites found to show excellent stability at lower and higher pH conditions providing scope for surface modification with biodegradable polymers to obtain biocompatible ferrite nanoparticles.

ACKNOWLEDGEMENTS

One of the authors, N. John Jebarathinam gratefully acknowledge to Jawaharlal Nehru Center for Advanced Scientific Research, Bangalore, India for recording FESEM micrograph, VSM and zeta potential analysis of the synthesized samples.

REFERENCES

1. M. Pardavi-Horvath, *J. Magn. Magn. Mater.*, **215-216**, 171 (2000); https://doi.org/10.1016/S0304-8853(00)00106-2.
2. N.A. Hill, *J. Chem. Phys. B*, **104**, 6694 (2000); https://doi.org/10.1021/jp000114x.
3. J.E.W. Verwey, *Nature*, **144**, 327 (1939); https://doi.org/10.1038/144327b0.
4. T. Goto, T. Kimura, G. Lawes, A.P. Ramirez and Y. Tokura, *Phys. Rev. Lett.*, **92**, 257201 (2004); https://doi.org/10.1103/PhysRevLett.92.257201.
5. M.H. Sousa, F.A. Tourinho, J. Depeyrot, G.H. da Silva and M.C.F.L. Lara, *J. Phys. Chem. B*, **105**, 1168 (2001); https://doi.org/10.1021/jp0039161.
6. F.H. Chen, L.M. Zhang, Q.T. Chen, Y. Zhang and Z.J. Zhang, *Chem. Commun.*, **46**, 8633 (2010); https://doi.org/10.1039/c0cc02577a.
7. Z. Zi, Y. Sun, X. Zhu, Z. Yang, J. Dai and W. Song, *J. Magn. Magn. Mater.*, **321**, 1251 (2009); https://doi.org/10.1016/j.jmmm.2008.11.004.
8. C. Liu, A.J. Rondinone and Z.J. Zhang, *Pure Appl. Chem.*, **72**, 37 (2000); https://doi.org/10.1351/pac200072010037.
9. A.B. Rajput, S. Hazra and N.N. Ghosh, *J. Exp. Nanosci.*, **8**, 629 (2013); https://doi.org/10.1080/17458080.2011.582170.
10. H.T. Rahal, R. Awad, A.M. Abdel-Gaber and D. El-Said Bakeer, *J. Nanomater.*, **Article ID 7460323** (2017); https://doi.org/10.1155/2017/7460323.
11. M. Sheikholeslami, *Eur. Phys. J. Plus*, **131**, 413 (2016); https://doi.org/10.1140/epjp/i2016-16413-y.
12. H. Xiang, Y. Mu, C. Hu and X. Luo, *J. Nanomater.*, **Article ID 5429063** (2017); https://doi.org/10.1155/2017/5429063.

13. X. Sun and S. Sun, *Methods Mol. Biol.*, **1570**, 73 (2017); https://doi.org/10.1007/978-1-4939-6840-4_5.
14. H. Chang and H.-T. Su, *Rev. Adv. Mater. Sci.*, **18**, 667 (2008).
15. R. Patil, S. Kakatkar, A. Sanlepal and S. Sawant, *J. Pure Appl. Phys.*, **2**, 193 (1994).
16. N.J. Jebarathinam, M. Eswaramoorthy and V. Krishnasamy, *Appl. Catal. A Gen.*, **145**, 57 (1996); https://doi.org/10.1016/0926-860X(96)00149-4.
17. K. Nejati and R. Zabihi, *Chem. Cent. J.*, **6**, 394 (2012); https://doi.org/10.1186/1752-153X-6-23.
18. A.S. Eggeman, A.K. Petford-Long, P.J. Dobson, J. Wiggins, T. Bromwich, R. Dunin-Borkowski and T. Kasama, *J. Magn. Magn. Mater.*, **301**, 336 (2006); https://doi.org/10.1016/j.jmmm.2005.07.022.
19. J.D. Byrne, T. Betancourt and L. Brannon-Peppas, *Adv. Drug Deliv. Rev.*, **60**, 1615 (2008); https://doi.org/10.1016/j.addr.2008.08.005.
20. Y. Obata, S. Tajima and S. Takeoka, *J. Control. Rel.e*, **142**, 267 (2010); https://doi.org/10.1016/j.jconrel.2009.10.023.